Helical light emission from plasmonic vortices via magnetic tapered tip

IOP Conf. Series: Journal of Physics: Conf. Series **961** (2018) 012001 doi:10.1088/1742-6596/961/1/012001

Helical light emission from plasmonic vortices via magnetic tapered tip

N Maccaferri[1*], Y Gorodetski[2], and D Garoli[1]

[1]Istituto Italiano di Tecnologia, Via Morego 16, 16136 Genova, Italy

[2]Mechanical Engineering Department and Electrical Engineering Department, Ariel University, 40700 Ariel, Israel

*nicolo.maccaferri@iit.it

Abstract. We investigate an architecture where a plasmonic vortex excited in a gold surface propagates on an adiabatically tapered magnetic tip and detaches to the far-field while carrying a well-defined optical angular momentum. We analyze the out-coming light and show that, despite generally high losses of flat magnetic surface, our 3D structure exhibits high energy throughput. Moreover, we show that once a magneto-optical activity is activated inside the magnetic tip a modulation of the total power transmittance is possible.

1. Introduction

Recently, structured optical beams became a subject of an intense research [1], due to numerous potential applications they offer in the fields of super-resolution imaging [2], optical tweezing [3], nanomanipulation [4] and telecommunications [5]. A special interest is dedicated to investigation of the interaction of structured light with metallic nanostructures, resulting in Surface Plasmon Polaritons (SPPs) carrying angular momentum (AM) [6–13]. These surface confined electromagnetic distributions are generally defined by a field singularity surrounded by a helical phase front, referred here as plasmonic vortices (PVs). The singularity strength is termed the topological charge of a vortex, and defined by the phase ramp acquired in one round trip about the singularity center. This charge is proportional to the orbital AM (OAM) carried by the field [9]. PVs are usually generated by coupling propagating vortex beams to the plasmonic mode on a metal surface by using center-symmetric coupling structure, known also as plasmonic vortex lenses (PVLs) [9]. A PVL generally comprises of periodic spiral or circular grooves or slits milled in the metal [6–9, 12–18]. The total AM of the resulting PV carries contributions from both the incident OAM and the additional OAM introduced by the coupling structure. Some more complex architectures proposed both coupling of light into a PV and then coupling of the propagating PV to the far-field, generating a scattered beam carrying non-zero orbital AM [6,8,15,16,18,19]. In this case, the PV generated by interaction of the incident light with a PVL can be modulated in the near-field and then scattered into free space by a proper decoupling structure. Most of the proposed systems utilized scattering as a primary coupling mechanism [6,16,19]. Although, it was shown that the latter method provides a way to abruptly modify the mode's AM it demonstrates a very low transmittance efficiency and not pure polarization state [19]. Recently we have experimentally demonstrated an efficient PV coupling to the free space by means of a single-layer PVL structure via adiabatically tapered gold tip at its center [6]. We have shown that by properly shaping the nanotip geometry the PV excited at the spiral structure can be coupled to far-field distribution carrying well defined OAM. Nevertheless, these effects can be solely controlled by the properly designed 3D shape of the tip and by the illuminating beam parameters. Various practical applications in nanophotonics require fast external control of the emerging beam characteristics. In this regard magnetoplasmonic devices draw a very promising route to active nanophotonics, since an externally applied magnetic field can alter the plasmonic response leading to novel and unexpected effects [20–29]. Obviously the main requirement of these devices is to be fabricated

from the material that has both good plasmonic and magnetic properties, for instance nickel or cobalt [22, 23]. Here we demonstrate an architecture where a plasmonic vortex excited by a PVL milled in a gold surface propagates on an adiabatically tapered magnetic tip and detaches to the far-field while carrying a well-defined OAM. We analyze the light transmittance and show that despite generally high losses of flat nickel surface our 3D structure exhibits relatively high energy thoughput providing optimistic forecast for active magnetically-driven photonics.

2. Numerical simulations

In Fig. 1(a) we depict a scheme of the proposed structure, which comprises a multiple-turn spiral slit milled on a 300 nm gold film deposited onto a 100 nm Si_3N_4 membrane and a conical metallic tip located exactly at the center of the spiral. In this work the tip is made of nickel and cobalt. We first assume zero magnetic field or magnetization within the magnetic tip, thus the dielectric constant of nickel and cobalt is given by a single complex scalar. In the last part we assume that a magnetic field is applied along the tip (z-direction) [30, 31]. Three main parameters define the tip shape, namely its height (h), aperture angle (α), and curvature radius at the basis (r_c). The curvature radius at the tip apex is kept fixed to 20 nm throughout the paper. It is worth mentioning that the fabrication technique developed in previous works [6] enables to faithfully reproduce the designed structure proposed here.

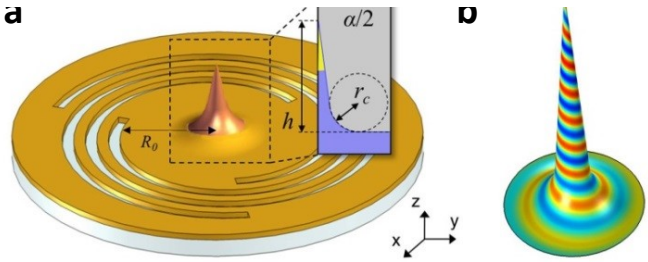

Fig. 1. (a) Scheme of the PVL. The geometrical parameters of the spiral slits are slit width = 200 nm, period= 763 nm, gold thickness = 100 nm, Si_3N_4 thickness = 100 nm. The nickel tip has h=6.5 μm; α=15° and r_c=1.57 μm. (b) Calculated z-component of the electric field propagating along the tip.

We analyze the case of a circularly polarized plane-wave impinging normally from the Si_3N_4 side. As has been described elsewhere [7–9,14], the electric field component locally orthogonal to the slits efficiently couples to the SPP mode of the metal-air interface. The plasmonic wavefronts launched by each spiral constructively interfere (the spiral period is λ_{SPP}) producing a PV radially propagating towards the PVL center. In the absence of the tip, the PV confined by the spiral grooves forms a standing wave, giving rise to the characteristic Bessel interference pattern [6]. The z-component of the electric field, in cylindrical coordinates, is proportional to $J_l(k_{SPP}r)exp(-\kappa z)$ $\exp(il\phi)$, where k_{SPP} is the wave vector of an SPP propagating on a flat gold-air interface, J_l is the lth order Bessel function of first kind and $\kappa = \sqrt{k_{SPP}^2 - k_0^2}$, where $k_0=2\pi/\lambda_0$ is the wave vector of light in vacuum. It can be shown that the PV carries an orbital OAM quanta of $l\hbar$ where l is the PV topological charge, given by $l = m + s_l$ with the incident spin number $s_l = \pm 1$ corresponding to the right hand and left hand circularly polarized light, respectively, and m defining the topological charge of the spiral [7–9,14]. When the conical tip is present at the PVL center the surface confined electromagnetic mode may couple to the guided mode propagating along the tip upwards. In [6] we compared the behaviors of the PV with $l = 1$ excited on two structures having similar conical tips but with different curvature radius at the basis. We have shown that in the case of the negligible curvature radius ($r_c \to 0$) most of the energy is reflected back while a small fraction of the incoming energy is scattered to the far-field from the tip base. By increasing of the curvature radius at the tip basis (in our design r_c = 1.57 μm) the scattering diminishes and the mode is smoothly guided towards the top of the tip, and the spiral phase-fronts of the PV propagate on the tip almost without the losses (see the E_z component of the plasmonic field simulated by the COMSOL Multiphysics® software in Fig. 1(b)). The smoothed tip in this configuration perfectly matches between the PV and the corresponding plasmonic mode of the conical waveguide. This guided mode experiences gradual acceleration due to a local increasing of the effective index, and at some height, where its momentum matches the one of the free-space radiation, it detaches to the far-field. This has been demonstrated, both by means of finite element simulations and experimental measurements for a gold

PVL and tip [6]. Here we replace, the gold tip with a magnetic one, made of nickel or cobalt. The use of a magnetic material implies potentially interesting effects turning our metal structure into an optically active device by applying an external magnetic field. In the following part we compare the behavior of the previously investigated gold structure with a similar structure where the tip is completely, or partially made of a magnetic material.

Figure 2 reports the |E| maps for the PVs with l = 0, 1, 2 and 3 for a tip made of nickel. As can be seen, the behavior is similar with respect to the gold tip reported in [6]. For l = 0 the PV propagates to the end of the tip and is almost perfectly reflected back, which can be deduced by observing the interference pattern along the metal surface. This is the only mode that experiences an increasing of the effective index and slows down along the tip giving rise to the mode localization at the tip apex. For l = 1 our nickel tip nicely guides the PV to the tip apex where it beams out as a perfect Gaussian source. For higher l (l > 1), the PVs are efficiently decoupled to the free space in lower points and characteristic doughnut shaped distributions are expected in the far-field.

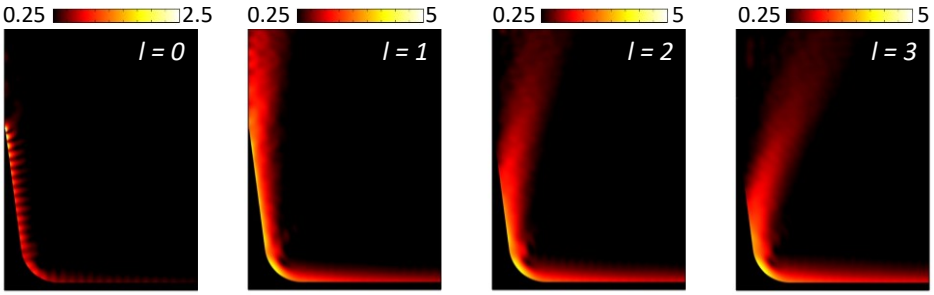

Fig. 2. |E| maps in case of a smoothed conical nickel tip illuminated by a PV with the indicated l values.

A smooth connection of the tip base insures almost lossless coupling of the plasmonic mode at the surface to the mode guided at the cone. The only losses in the system are attributed to the plasmonic absorption in the metal. By replacing the gold with nickel we introduce higher ohmic losses, however as can be seen in Fig. 2 the system still produces relatively efficient beaming. In Fig. 3(a) we summarize the PV total power transmittance as a function of l for various configurations comprising Au, Ni and Co tip. The transmittance efficiency spans from 10% for l = 1 PV and up to 35% at l = 5. In a comparison with the transmittance efficiency of the recently proposed holey PVL (5%) [19] our device shows a clear improvement while keeping the ability of far-field AM beaming.

In order to better investigate the transmittance efficiency of a Ni tip we performed the simulations where the tip is only partially covered with Ni. In Fig. 3(b) the transmittance of our structure for the cases of l = 0 and l = 1 are reported as a function of the height (y) of Au (see the inset of Fig.3(b)). As expected the transmittance increase rapidly when the Au coverage grows. The last point corresponds to the situation when only the final 1.5 μm of the tip apex are covered with the nickel. As recently discussed [6, 31], the tip profile we presented was optimized to maximize not only the transmittance, but also the polarization contrast. The latter was defined as $Q = 1 - P_+/P_-$, with P_+ and P_- being the light powers decoupled by the tip with right and left circular polarization state, respectively. Here we want to study this behavior when the Au tip is replaced by a magnetic one. Plots of Q are reported in Fig. 3(c) and (d). As expected, due to higher losses, Q values with the magnetic tips are lower respect to the case of a gold tip. This can be explained by a plasmon depolarization due to the high losses imposing short coherence length. To be specific, the calculated coherence length of a plasmonic wave on a flat magnetic is ~*3* μm, which is roughly a half of the total cone length. As can be seen in Fig. 3(b) Q increases with the PV l order due to the corresponding detachment height decrease. The Q drops again for the PV with l = 4 due to a broad spatial divergence of the beam and an additional scattering from Au slab/magnetic tip interface.

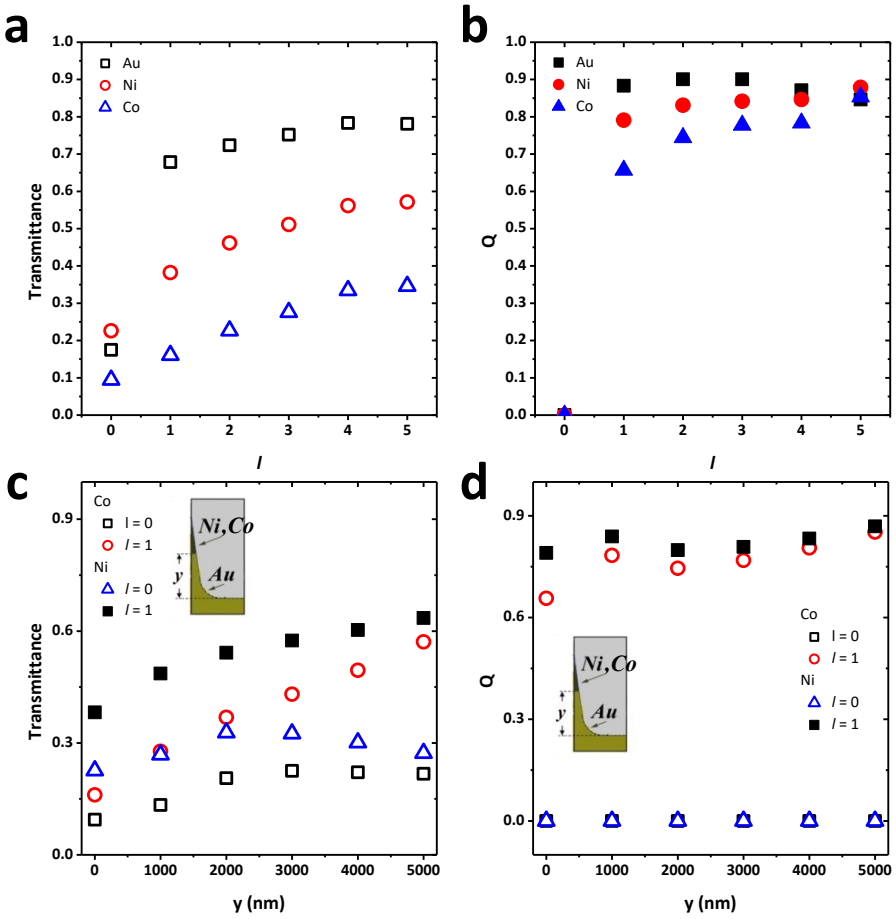

Fig. 3. Comparison of the far-field transmittance (a) and polarization contrast Q (b) obtained from the magnetics tip compared with data obtained with a gold nanostructure [6]; Tip transmittance (c) and Q (d) when the magnetic material covers the upper part of the tip starting from a height denoted by y (see the insets). Computation from $y = 0$ nm (the whole tip is covered by Nickel) to y = 5000 nm (only the upper 1.5 μm of the tip is covered by Ni or Co).

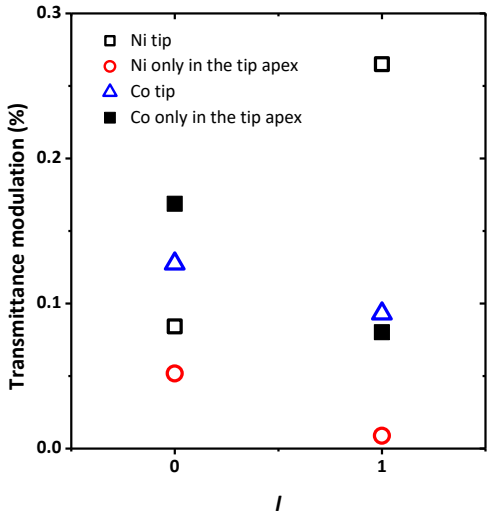

Fig. 4. Magnetic modulation of the total power transmittance for $l = 0$ and 1.

Finally, we study the effect of the application of an external magnetic field. In this case the dielctric tensor of the magnetic material is no more diagonal [30,31]. In Fig. 4 we show the magnetic modulation of the total power transmittance for the cases $l = 0,1$ for both Co and Ni tip, and for the cases where only the final 1.5 μm of the tip apex is covered with the magnetic material. The magnetic modulation is defined as [2*(T(+H)-T(-H))/ (T(+H)+T(-H))]. As it can be seen the modulation is below 1% in all the cases. It is worth noticing that, while in the Ni case covering just the tip apex gives a smaller modulation for both the values of the topological charge considered here, in the Co case the modulation is higher for $l = 0$ when we cover only the tip apex with the magnetic material. Moreover, for $l = 1$, in the Ni case we have almost zero modulation if we cover only the tip apex, while in the case of a pure Ni tip we observe a modulation of almost 0.6%. In the Co case we do not observe a huge change if we have a pure Co tip or a gold tip covered with Co only on the apex. This latter case is interesting because one can use a tip made of pure gold and cover it only in the apex with the magnetic material, thus retaining the good transmittance efficiency (>50%) while maintaining a magnetic modulation functionality. To improve the modulation one can use magnetic materials with a strong magneto-optical activity, such as CoFeTb [31]. The proper design of the system, however, should consider simultaneously optimizing the magnetic and the plasmonic properties of the material. Using these considerations the conical tip structure can be further optimized.

3. Conclusions

In summary, we studied a plasmonic vortex lens structure capable of coupling a circularly polarized light to a plasmonic vortex and efficiently transmitting it to the far-field by means of a smoothed-cone magnetic tip placed at its center. As for the case of Au tip, the large curvature radius at the cone basis was shown to play a crucial role in enabling an adiabatic coupling of the plasmonic vortex propagating on the flat metal surface to the plasmonic modes of the metal tip, whose tapering, in turn, enables an adiabatic match to the propagating waves in free space. The higher losses related to the use of a magnetic material lead to lower transmitted power to the far-field although the beaming is preserved. Changing the configuration by partially covering a Au tip with Ni or Co (on the tapered) can increase significantly the efficiency of the structure. Finally, this particular design shows interesting behaviours when the polarization contrast is evaluated. Finally the magneto-optical modulation effects shown here, once an external magnetic field is applied, suggest intriguing active optical phenomena.

References

[1] Cardano F, and Marrucci L 2015 *Nat. Photonics* **9** 776–778
[2] Tamburini F, Anzolin G, Umbriaco G, Bianchini A, and Barbieri C 2006 *Phys. Rev. Lett.* **97** 163903
[3] Padgett M, and Bowman R 2011 *Nat. Photonics* **5** 343–348
[4] Toyoda K, Miyamoto K, Aoki N, Morita R, and Omatsu T 2012 *Nano Lett.* **12** 3645–3649
[5] Bozinovic N, Yue Y, Ren Y, Tur M, Kristensen P, Huang H, Willner A E, and Ramachandran S 2013 *Science* **340** 1545–1548
[6] Garoli D, Zilio P, Gorodetski Y, Tantussi F, and De Angelis F 2016 *Nano Lett.* ***16*** 6636-6643
[7] Gorodetski Y, Niv A, Kleiner V, and Hasman E 2008 *Phys. Rev. Lett.* **101** 043903
[8] Gorodetski Y, Shitrit N, Bretner I, Kleiner V, and Hasman E 2009 *Nano Lett.* **9** 3016–3019
[9] Kim H, Park J, Cho S, Lee S, Kang M, and Lee B 2010 *Nano Lett.* **10** 529–536
[10] Bliokh K Y, Rodríguez-Fortuño F J, Nori F, and Zayats A V 2015 *Nat. Photonics* **9** 796–808
[11] Miao J, Wang Y, Guo C, Tian Y, Zhang J, Liu Q, Zhou Z, and Misawa H 2011 *Plasmonics* **7** 377–381
[12] Chen W, Abeysinghe D C, Nelson R L, and Zhan Q 2010 *Nano Lett.* **10** 2075–2079
[13] Cho S-W, Park J, Lee S-Y, Kim H, and Lee B 2012 *Opt. Express* **20** 10083–10094
[14] Zilio P, Mari E, Parisi G, Tamburini F, and Romanato F 2012 *Opt. Lett.* **37** 3234–3234
[15] Zilio P, Parisi G, Garoli D, Carli M, and Romanato F 2014 *Opt. Lett.* **39** 4899–902
[16]Yu H, Zhang H, Wang Y, Han S, Yang H, Xu X, Wang Z, Petrov V, Wang J 2013 *Sci. Rep.* **3** 3191
[17] Genevet P, Lin J, Kats M A, and Capasso F 2012 *Nat. Commun.* **3** 1278
[18] Garoli D, Zilio P, Gorodetski Y, Tantussi F, and De Angelis F 2016 *Sci. Rep.* **6** 29547
[19] Gorodetski Y, Drezet A, Genet C, and Ebbesen T W 2013 *Phys. Rev. Lett.* **110** 203906

[20] Temnov V V 2012 *Nat. Photonics* **6** 728
[21] Armelles G, Cebollada A, García-Martín A, and Ujué González M 2013 *Adv. Opt. Mater.* **1** 10
[22] Maccaferri N, Berger A, Bonetti S, Bonanni V, Kataja M, Hang Qin Q, van Dijken S, Pirzadeh Z, Dmitriev A, Nogués J, Åkerman J, and Vavassori P 2013 *Phys. Rev. Lett.* **111** 167401
[23] Lodewijks K, Maccaferri N, Pakizeh T, Dumas R K, Zubritskaya I, Åkerman J, Vavassori P, and Dmitriev A 2014 *Nano Lett.* **14** 7207–7214
[24] Maccaferri N, Kataja M, Bonanni V, Bonetti S, Pirzadeh Z, Dmitriev A, van Dijken S, Åkerman J, Vavassori P 2014 *Phys. Status Solidi A* **211** 1067-1075
[25] Maccaferri N, Gregorczyk K E, de Oliveira T V A G, Kataja M, van Dijken S, Pirzadeh Z, Dmitriev A, Åkerman J, Knez M, Vavassori P 2015 *Nat. Commun.* **6** 6150
[26] Zubritskaya I, Lodewijks K, Maccaferri N, Mekonnen A, Dumas R K, Åkerman J, Vavassori P, Dmitriev A 2015 *Nano Lett.* **15** 3204–3211
[27] Maccaferri N, Inchausti X, García-Martín A, Cuevas J C, Tripathy D, Adeyeye A O, Vavassori P 2015 *ACS Photonics* **2** 1769-1779
[28] Kataja M, Pourjamal S, Maccaferri N, Vavassori P, Hakala T K, Huttunen M J, Törmä P, van Dijken S 2016 *Opt. Express* **24** 3652-3662
[29] Maccaferri N, Bergamini L, Pancaldi M, Schmidt M, Kataja M, van Dijken S, Zabala N, Aizpurua J, Vavassori P 2016 *Nano Lett.* **16** 2533-2542
[30] Maccaferri N, González-Díaz J B, Bonetti S, Berger A, Kataja M, van Dijken S, Nogués J, Bonanni V, Pirzadeh Z, Dmitriev A, Åkerman J, Vavassori P 2013 *Opt. Express* **21** 9875-9889
[31] Maccaferri N, Gorodetski Y, Toma A, Zilio P, De Angelis F, Garoli D 2017 *Appl. Phys. Lett.* **111** 201104